



OPEN ACCESS

EDITED BY

Daniele Sblattero,
University of Trieste, Italy

REVIEWED BY

Xiaojie Chu,
University of Pittsburgh, United States
Shambojit Roy,
Birla Institute of Technology and Science,
India
Molly Shoichet,
University of Toronto, Canada

*CORRESPONDENCE

John Löfblom
[✉ lofblom@kth.se](mailto:lofblom@kth.se)

RECEIVED 24 May 2024

ACCEPTED 23 July 2024

PUBLISHED 08 August 2024

CITATION

Ek M, Nilvebrant J, Nygren P-Å, Ståhl S,
Lindberg H and Löfblom J (2024) An anti-
sortilin affibody-peptide fusion inhibits
sortilin-mediated progranulin degradation.
Front. Immunol. 15:1437886.
doi: 10.3389/fimmu.2024.1437886

COPYRIGHT

© 2024 Ek, Nilvebrant, Nygren, Ståhl, Lindberg
and Löfblom. This is an open-access article
distributed under the terms of the [Creative
Commons Attribution License \(CC BY\)](https://creativecommons.org/licenses/by/4.0/). The
use, distribution or reproduction in other
forums is permitted, provided the original
author(s) and the copyright owner(s) are
credited and that the original publication in
this journal is cited, in accordance with
accepted academic practice. No use,
distribution or reproduction is permitted
which does not comply with these terms.

An anti-sortilin affibody-peptide fusion inhibits sortilin-mediated progranulin degradation

Moira Ek, Johan Nilvebrant, Per-Åke Nygren, Stefan Ståhl,
Hanna Lindberg and John Löfblom*

Department of Protein Science, School of Engineering Sciences in Chemistry, Biotechnology and Health, KTH Royal Institute of Technology, Stockholm, Sweden

Heterozygous loss-of-function mutations in the *GRN* gene are a common cause of frontotemporal dementia. Such mutations lead to decreased plasma and cerebrospinal fluid levels of progranulin (PGRN), a neurotrophic factor with lysosomal functions. Sortilin is a negative regulator of extracellular PGRN levels and has shown promise as a therapeutic target for frontotemporal dementia, enabling increased extracellular PGRN levels through inhibition of sortilin-mediated PGRN degradation. Here we report the development of a high-affinity sortilin-binding affibody-peptide fusion construct capable of increasing extracellular PGRN levels *in vitro*. By genetic fusion of a sortilin-binding affibody generated through phage display and a peptide derived from the progranulin C-terminus, an affinity protein (A3-PGRN_C15*) with 185-pM affinity for sortilin was obtained. Treating PGRN-secreting and sortilin-expressing human glioblastoma U-251 cells with the fusion protein increased extracellular PGRN levels up to 2.5-fold, with an EC₅₀ value of 1.3 nM. Our results introduce A3-PGRN_C15* as a promising new agent with therapeutic potential for the treatment of frontotemporal dementia. Furthermore, the work highlights means to increase binding affinity through synergistic contribution from two orthogonal polypeptide units.

KEYWORDS

protein engineering, affibody molecule, sortilin (SORT1), progranulin (GRN), frontotemporal dementia (FTD), latozinemab, phage display

Abbreviations: ABD, Albumin-binding domain; AD, Alzheimer's disease; BSA, Bovine serum albumin; CD, Circular dichroism; FTD, Frontotemporal dementia; HSA, Human serum albumin; IMAC, Immobilized metal affinity chromatography; MS, Mass spectrometry; NT, Neurotensin; PBS, Phosphate-buffered saline; PGRN, Progranulin; SPR, Surface plasmon resonance.

1 Introduction

Frontotemporal dementia (FTD) is a form of non-Alzheimer's dementia that is particularly common among cases of early-onset dementia (1). The disease is characterized by atrophy of the frontal and temporal lobes of the brain (2), leading to one of three main clinical phenotypes, with symptoms ranging from behavioral changes to language impairments (3). On a molecular level, FTD is characterized by aggregation of either microtubule-associated protein tau (MAPT), TAR DNA-binding protein 43 (TDP-43), or fused-in-sarcoma (FUS) (3).

The disease has a strong genetic component, and a family history of FTD is present in up to 40% of all cases (4–6). The majority of these cases are due to mutations in the genes encoding either microtubule-associated protein tau (MAPT), progranulin (GRN), or chromosome 9 open reading frame 72 (C9orf72) (7). Heterozygous mutations in the GRN gene, encoding the protein progranulin (PGRN), are present in about 5–10% of all FTD cases, and up to 26% of familial FTD cases (4, 8–11). To date, at least 130 different disease-associated mutations have been identified in the GRN gene (7).

PGRN is a 593-amino acid glycoprotein consisting of seven and a half cysteine-rich granulin domains (12–14), into which the protein can be cleaved by both intra- and extracellular proteases (15, 16). PGRN and the different granulins exert a multitude of, sometimes opposing (16), functions, including roles in lysosomal function (17, 18) and as a neurotrophic factor (19–21). The identified pathogenic mutations in the GRN gene are believed to cause FTD through haploinsufficiency (9, 22), as they are associated with more than 50% decreased PGRN levels in plasma and CSF of mutation carriers compared to controls (19, 23–25). Thus, increasing PGRN levels to the normal range is currently investigated as a potential therapeutic strategy for the treatment of FTD with GRN mutations (FTD-GRN).

An interesting target to this end is the PGRN clearance receptor, sortilin. This is a type I membrane protein, with the main luminal domain forming a 10-bladed beta propeller with an inner tunnel into which both PGRN and the neuropeptide neurotensin (NT) bind (26–29). PGRN interacts with sortilin through the PGRN C-terminal tail, leading to endocytosis and lysosomal localization of PGRN (28, 29). Thus, sortilin is a negative regulator of extracellular PGRN levels (28, 30). Importantly, the neurotrophic effects of PGRN have been shown to be independent of sortilin binding (20, 21), making sortilin an attractive target for efforts to increase extracellular PGRN levels. Blocking the PGRN-sortilin interaction has been demonstrated to increase PGRN levels *in vitro* and *in vivo* in several studies (31–33). Most notably, the anti-sortilin IgG1 latozinemab (32) is currently in phase 3 clinical trials for FTD-GRN (clinicaltrials.gov ID: NCT04374136), establishing sortilin targeting as a promising treatment strategy for FTD-GRN.

As an alternative to antibodies, targeted therapies can also be based on smaller engineered antibody domains or non-Ig-derived alternative scaffold proteins (34), possessing several potential advantages over antibodies in cases where Fc-mediated effector

functions are undesirable. One such class of alternative scaffold proteins is affibody molecules. These are small (58-amino acid, ~6.5 kDa) three-helical affinity proteins based on the Z domain, a derivative of *Staphylococcus aureus* protein A (35, 36). Typically, 13 or 14 surface-exposed positions in helix 1 and 2 are randomized to generate a library from which affibody molecules with affinity for new targets can be selected (37) (Figure 1A). In comparison to antibodies, the affibody scaffold notably lacks inherent effector functions, as well as disulfide bonds, and generally benefits from high stability. Its small size also makes it amenable to production in bacterial hosts or through chemical synthesis. The small size has furthermore prompted modular approaches, such as tandem fusions of several affibody molecules to increase target affinity (38), fusion of affibody molecules to enzymes (39, 40) or anti-idiotypic affibody molecules (41, 42) in prodrug approaches, or fusion with albumin-binding domains (ABD) for half-life extension *in vivo* (43). An IL-17A-targeting, ABD-containing affibody construct is currently being investigated in phase 3 clinical trials (NCT05623345, NCT05905783), having demonstrated good safety and tolerability in humans (44).

Here, we introduce a novel affibody-based sortilin-targeting approach for increasing extracellular PGRN levels. First, sortilin-specific affibody molecules were selected using phage display technology. We next explored genetic fusions of several affibody candidates to short peptides derived from the sortilin-binding C-terminal part of PGRN, to possibly increase affinity via synergistic binding. The most optimal fusion construct resulted in a dramatic increase (>380-fold) in binding affinity to sortilin and was shown to increase extracellular PGRN levels *in vitro* in sortilin-expressing, PGRN-secreting human glioblastoma U-251 cells, with an EC₅₀ comparable to that of latozinemab, suggesting a therapeutic potential. Further, this is the first example of a modular approach where fusion of an affibody molecule to a natural peptide targeting the same receptor leads to greatly improved affinity and biological activity.

2 Materials and methods

2.1 Labeling of targets and secondary reagents

Murine (R&D Systems, 2934-ST) and human (R&D Systems, 3154-ST) sortilin proteins were biotinylated for 1 h using EZ-Link Sulfo-NHS-LC-Biotin (Thermo Fisher Scientific) in a 25-fold molar excess followed by dialysis to PBS using a Slide-A-Lyzer 10K MWCO (Thermo Fisher Scientific). Human serum albumin (HSA, 20 mg/ml) was labeled with Alexa FluorTM 647 succinimidyl ester (Invitrogen A-20006, 0.5 mg/ml) in carbonate buffer (0.1 M, pH 8.5) for 3 hours at room temperature, followed by quenching with a 1000-fold molar excess of glycine. Labeled HSA was purified by gel filtration into PBS (pH 7.4) using PD-10 columns (Cytiva), according to the manufacturer's instructions. Concentration of the proteins was determined using absorbance at 280 nm.

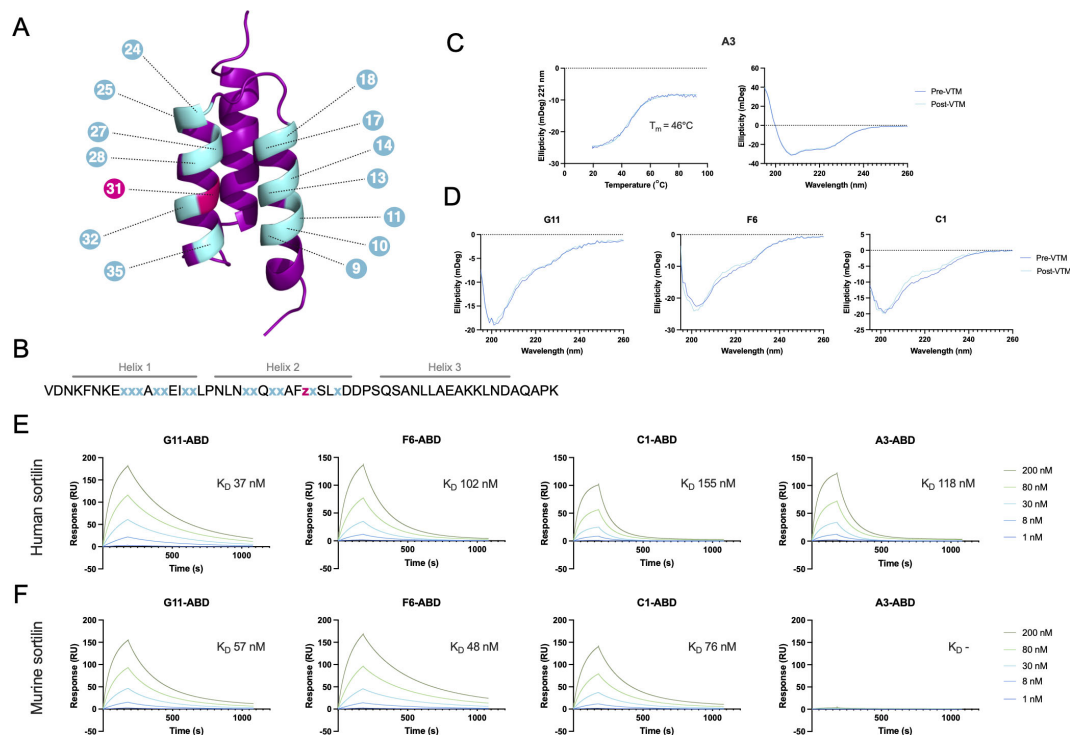


FIGURE 1

Schematic overview of the affibody scaffold and initial characterization of anti-sortilin affibodies. (A, B) Schematic of a three-helical affibody molecule (A) and the sequence of the affibody scaffold (B), highlighting the 14 randomized positions in the phage display library. Gray lines over the sequence indicate the expected positions of the three alpha helices. Randomized positions are shown in cyan (x), indicating an equal mixture of all amino acids excluding Cys and Pro, or pink (z), indicating a distribution with 60% Ile and 10% each of His, Tyr, Lys, and Asp. (C) Circular dichroism spectroscopy of the anti-sortilin affibody variant A3, including variable temperature measurements (VTM) at 221 nm (left), and secondary structure determination before and after thermal melting (right). VTM measurements are shown in dark blue, with the 4-parameter curve fit from which the melting temperature was estimated shown in turquoise. (D) Circular dichroism spectroscopy of the anti-sortilin affibody variants G11, F6 and C1, showing secondary structure determination before and after thermal melting. (E, F) Surface plasmon resonance (SPR) sensorgrams showing the interaction between the anti-sortilin affibodies and human (E) or murine (F) sortilin. Affibody-ABD fusion proteins were captured on a sensor chip surface functionalized with HSA, followed by injection of sortilin, as indicated in the figure. Inserts indicate the equilibrium dissociation constant for the interaction between the respective affibody and sortilin, as estimated by a 1:1 Langmuir model fit.

2.2 Phage display selection of anti-sortilin affibody molecules

Phage display selections of affibodies binding to sortilin were performed essentially as described by Giang et al. (45), using a previously described combinatorial phage library of the Z domain with randomization in 14 positions (46) (Figures 1A, B). Briefly, four cycles of bio-panning were conducted at room temperature in PBSTB (PBS with 0.1% Tween20 and 3% w/v BSA) with decreasing target concentration and increasing washing in each round. In the first two cycles, biotinylated sortilin was pre-immobilized onto paramagnetic streptavidin beads (M-280, Thermo Fisher Scientific) and in the later cycles, phages were incubated with biotinylated target in solution before capture of target-phage complexes on beads. Parallel selections were performed using either murine or human sortilin as target, and bound phages were eluted by either trypsin cleavage (Gibco by Life Technologies, #15090-046, 2.5 mg/ml) or acid (0.3 M HAc, pH 2.8). Starting in the third round, two additional selection tracks were initiated from pooled phage stocks from the two elution strategies for each target (murine/human sortilin) and subjected to competitive elution (1 h

incubation) using 5 μ M neurotensin (Sigma, N6383) in PBST (PBS supplemented with 0.05% Tween20, pH 7.4). 47 random clones from each of the six selection tracks were assayed by phage-ELISA for binding to human and murine sortilin (immobilized in separate wells at 2.5 μ g/ml in 0.1 M carbonate buffer pH 9.6). Binding signal from an albumin-binding domain (ABD_{wt}) tag fused to the C-terminus of phage p3-displayed affibody to immobilized HSA was used to normalize binding signals in ELISA (45). Clones with positive ELISA-signals were sent for sequencing.

2.3 Production and purification of recombinant proteins

Constructs of the format His₆-Z (Z) were cloned into a pT7 vector. First- and second-generation construct genes containing an ABD035 (47) (Supplementary Table S1) were synthesized as gene fragments and cloned into a pET21 expression vector (Twist Bioscience, South San Francisco, CA, USA) with an N-terminal hexahistidine tag for immobilized metal affinity chromatography (IMAC) purification. Constructs were of the formats His₆-Z-G₄S-

ABD035 (Z-ABD), His₆-Z-G₄S-ABD035-PGRN_C21* (Z-ABD-PGRN_C21*), His₆-ABD035-G₄S-Z-PGRN_C21* (ABD-Z-PGRN_C21*), His₆-ABD035-PGRN_C21* (ABD-PGRN_C21*), His₆-ABD035-G₄S-A3-PGRN_CX* (ABD-A3-PGRN_CX*), His₆-ABD035-G₄S-A3-(G₄S)₃-PGRN_CX* (ABD-A3-(G₄S)₃-PGRN_CX*), and His₆-ABD035-G₄S-A3-(G₄S)₃-NT_C3 (ABD-A3-(G₄S)₃-NT_C3). Plasmids were transformed into *Escherichia coli* BL21 Star cells (Thermo Fisher Scientific) using a standard heat shock transformation protocol, followed by protein production and purification. Briefly, cells were cultivated in tryptic soy broth with yeast extract (TSB+Y, Merck) supplemented with 100 µg/ml of carbenicillin or 50 µg/ml of kanamycin at 37°C and 150 rpm shaking. At an OD₆₀₀ of approximately 0.7, protein expression was induced with isopropyl β-D-1-thiogalactopyranoside (IPTG) to a final concentration of 1 mM. The cultures were incubated at 25°C and 150 rpm for approximately 16 hours prior to harvest. Cells were lysed by sonication, and proteins were purified by native IMAC on HisPur Cobalt Resin (Thermo Fisher Scientific) at 4°C. Purified proteins were buffer-exchanged to PBS (pH 7.4) using PD-10 columns (Cytiva), according to the manufacturer's recommendations, and analyzed by SDS-PAGE (NuPAGE, Invitrogen), bicinchoninic acid assay (Pierce, Thermo Fisher Scientific) and mass spectrometry (MS, 4800 MALDI TOF/TOF, Applied Biosystems/MDS SCIEX). Z-ABD format proteins were analyzed by size exclusion chromatography (Superdex 75 Increase 5/150 GL, Cytiva).

2.4 Surface plasmon resonance for affibody screening and affinity determination

Target binding was assessed by surface plasmon resonance (SPR) using Biacore 3000 (screening of affibody clones after phage display selections), Biacore T200 (screening of first-generation affibody-PGRN fusion constructs), and Biacore 8K (affinity determination of second-generation affibody-PGRN fusion constructs) instruments (Cytiva, Uppsala, Sweden), respectively. In all cases, HSA was immobilized through amine coupling on a CM5 sensor chip according to the manufacturer's recommendations, using 10 mM sodium acetate pH 4.5 as the immobilization buffer, with a reference surface being only activated and inactivated. PBST was used as the running buffer in all binding experiments. 30-100 RU of ABD035-containing constructs were captured on the HSA surface, followed by injection of 1-200 nM human (R&D Systems 3154-ST) or murine (R&D Systems 2934-ST) sortilin for 180 s at 30 µl/min and 25°C. Dissociation was recorded for 15 min (screening experiments) or 60 min (affinity determination experiments) prior to regeneration with 10 mM HCl for 30 s at 30 µl/min. Kinetic constants were estimated using 1:1 Langmuir curve fits of sensorgrams from which a reference capture of the respective ABD035-containing construct with a 0 nM sortilin injection had been subtracted.

2.5 Circular dichroism spectroscopy for secondary structure and melting temperature determination

Circular dichroism (CD) spectroscopy was performed on affibody molecules in a His₆-Z format to verify the secondary structure content, using a Chirascan Circular Dichroism Spectrometer (Applied Biophysics Ltd, Leatherhead, UK). All analyses were performed at a concentration of 0.1-0.2 mg/ml in PBS (pH 7.4) and a 1 mm path length. Secondary structure content was assessed by measuring ellipticity at 20°C from 195 nm to 260 nm. For alpha helical molecules, the thermal stability was evaluated by measuring the change in ellipticity at 221 nm when heating from 20°C to 95°C at 5°C/min. After cooling to 20°C, another spectrum was recorded (195-260 nm) to assess refolding capacity. The melting temperature (T_m) was obtained as the inflection point of a 4-parameter fit of the variable temperature measurement data in Prism version 10 (GraphPad, Boston, MA, USA).

2.6 Mammalian cell cultivation

U-251 (JCRB IFO50288) human glioblastoma cells were cultivated in Minimum Essential Medium with glutamine (Gibco MEM, Thermo Fisher Scientific 31095) supplemented with 10% fetal bovine serum (FBS, Gibco, Fisher Scientific). PC-3 (ATCC CRL-1435) human prostatic adenocarcinoma cells were cultivated in Roswell Park Memorial Institute 1640 medium with glutamine (Gibco RPMI 1640, Thermo Fisher Scientific 21875) supplemented with 10% FBS. Cells were grown at 37°C in a 5% CO₂ atmosphere and were detached from culture flasks using TrypLE™ EXPRESS (Thermo Fisher Scientific 12605), according to the supplier's recommendations.

2.7 Flow cytometric analysis of sortilin binding on U-251 and PC-3 cells

Primary constructs were pre-incubated with secondary constructs in PBS+1% BSA on ice for a minimum of 1 hour prior to their addition to cells. ABD035-containing constructs (100 nM) were pre-incubated with HSA-Alexa Fluor 647 (200 nM), and a positive control Human Sortilin Antibody (R&D systems MAB31541, 0.625 µg/ml) was pre-incubated with Alexa Fluor 647 Goat Anti-Mouse Antibody (Invitrogen A21235, 2.86 µg/ml). 2×10⁵ U-251 or PC-3 cells per sample were washed in 200 µl ice-cold PBS +1% BSA, followed by incubation with 200 µl pre-incubated affibody construct or control antibody for 40 min at 4°C. Cells were washed twice, followed by resuspension in 200 µl ice-cold PBS +1% BSA for analysis on a Cytoflex S flow cytometer (Beckman Coulter, Brea, CA, USA), gating single cells based on forward/side scatter, and using a 638 nm laser for fluorophore excitation and a 660/10 BP filter for detection.

2.8 PGRN clearance assay

A PGRN clearance assay was performed essentially as described by Miyakawa et al. (31). Briefly, 1×10^4 U-251 cells in 100 μ l of the appropriate medium were seeded per well of a 96-well plate (NuncTM Delta Surface, Thermo Fisher Scientific). The cells were incubated for 24 h prior to the addition of fresh medium containing different concentrations of protein constructs, in triplicates. After 72 h, supernatants were collected, and PGRN concentrations were quantified using Human Progranulin DuoSet ELISA (R&D Systems DY2420), according to the manufacturer's instructions. Absorbance was measured at 450 and 540 nm using a ClarioStar (BMG Labtech, Ortenberg, Germany) plate reader, and PGRN levels were normalized against untreated cells to obtain the PGRN level fold change upon treatment. EC₅₀ values were obtained from a 4-parameter fit in Prism version 10 (GraphPad, Boston, MA, USA). Means and standard deviations were calculated from the EC₅₀ values from N=3 independent experiments. In addition to in-house-produced affibodies and affibody-peptide fusion proteins, a latozinemab biosimilar (ProteoGenix PX-TA1676) was evaluated. The statistical significance of the difference in EC₅₀ values between ABD-A3-PGRN_{C15}* and latozinemab was evaluated using a paired two-tailed t-test in Prism version 10.

3 Results

3.1 Isolation of sortilin-binding affibody molecules through phage display

In order to obtain sortilin-binding affibody molecules, phage display selections were performed against human and murine sortilin. A previously described (45) M13 filamentous phage library of 3×10^{10} affibody variants with randomizations in 14 positions (Figures 1A, B) was subjected to four rounds of panning against decreasing concentrations of either human or murine sortilin. Target-binding clones were identified by phage ELISA-screening of a total of 282 randomly selected clones. DNA sequencing of 54 target-binding clones showed 31 unique sequences. Among these, 12 clones representing major sequence clusters were chosen for subcloning to a His₆-Z-ABD_{wt} format, expressed in *E. coli*, and purified by IMAC. After screening by surface plasmon resonance (SPR, data not shown), clones G11 (mSort track), F6 (mSort track), C1 (mSort track), and A3 (hSort track) were chosen for further characterization.

3.2 Production and characterization of sortilin-binding affibody molecules

The anti-sortilin affibody clones G11, F6, C1 and A3 were produced in soluble format in *E. coli*, in Z-ABD and Z formats. Following IMAC purification, >95% affibody monomeric state was confirmed by size exclusion chromatography of Z-ABD format proteins (Supplementary Figure S1), and the secondary structure

and thermal stability of the affibody molecules was investigated using circular dichroism spectroscopy of Z format proteins. Interestingly, only variant A3 displayed an expected alpha helical structure content. Variable temperature measurements of A3 showed a melting temperature (T_m) of 46°C, and complete refolding after heat treatment (Figure 1C). Variants G11, F6, and C1 showed CD spectra largely consistent with a random coil conformation (Figure 1D).

The affinity of the affibody molecules to human and murine sortilin was assessed by SPR, by capturing Z-ABD constructs on a sensor chip immobilized with HSA, followed by injection of five concentrations (ranging from 1 nM to 200 nM) of human and murine sortilin, respectively. No sortilin binding was observed to the negative control Z_{wt}-ABD construct, confirming the absence of potential interaction between sortilin and the ABD or the affibody scaffold. Interestingly, the three affibody candidates selected against murine sortilin (G11, F6 and C1) showed binding to both human and murine sortilin, whereas clone A3 only displayed binding to human sortilin (Figures 1E, F). The equilibrium dissociation constants (K_D) were in the range of 37 to 155 nM and 48 to 76 nM for human and murine sortilin, respectively.

3.3 Design of first-generation affibody-PGRN fusion constructs

The sortilin-progranulin interaction is known to be mediated by the C-terminal tail of PGRN (28, 29), and previous studies have reported that the three last amino acids in the C-terminus (QLL) are essential for binding to sortilin (29). Thus, it was hypothesized that a peptide derived from the PGRN C-terminus might be used as an extension to a sortilin-binding affibody to obtain a biparatopic sortilin-binding fusion protein. To test this hypothesis, fusion proteins of the four sortilin-binding affibodies and the human PGRN C-terminus were created (Figure 2A).

Previous work has demonstrated that the 24 last amino acids of PGRN (T570-L593, here denoted PGRN_{C24}) are sufficient for full binding to sortilin, whereas shorter versions PGRN_{C9} (R585-L593) and PGRN_{C6} (A588-L593) were found to interact with sortilin to a lesser extent (29). As amino acid 22 from the PGRN C-terminus is a cysteine (C572), PGRN_{C21} (L573-L593) was selected for the initial affibody-PGRN fusion proteins in order to avoid disulfide bond formation (Figure 2C). In addition, others have shown that an A588G mutation in PGRN increases proteolytic stability by disruption of a neutrophil elastase cleavage site, with no effect on PGRN uptake by cells (33). The A588G mutation was confirmed to not affect sortilin binding by SPR (data not shown), and the PGRN_{C21} peptide carrying the A588G mutation (henceforth PGRN_{C21}*) was chosen as the initial PGRN peptide moiety for fusion. Given that a free PGRN C-terminus has been shown to be required for sortilin binding (21, 29) and that the binding epitopes of the affibodies on sortilin were not known, we designed a set of eight fusion constructs with the ABD moiety located either N-terminally or between the affibody and PGRN peptide, to serve as a spacer (Figure 2A).

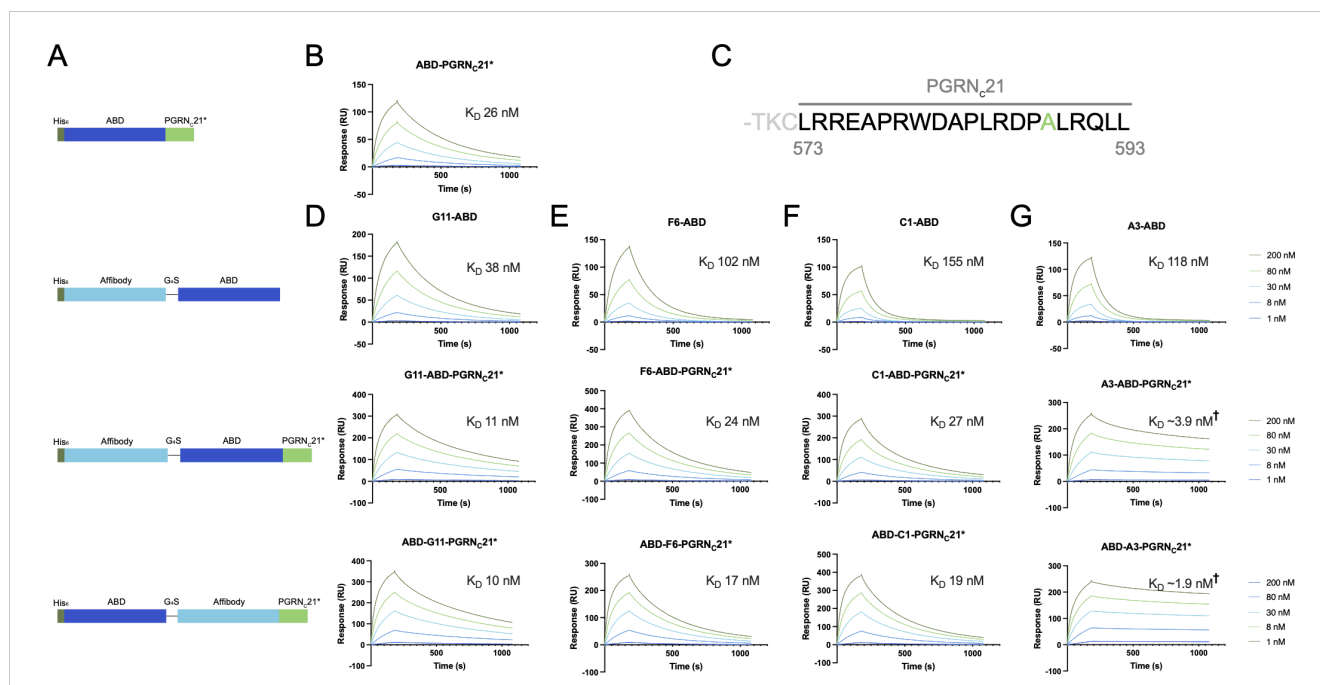


FIGURE 2

SPR screening of first-generation affibody-PGRN_C21* fusion proteins. (A) Schematic overview of the evaluated constructs. In addition to Z-ABD-PGRN_C21* and ABD-Z-PGRN_C21* format constructs, Z-ABD and ABD-PGRN_C21* constructs were included as controls. (B) SPR sensorgram showing the interaction between the PGRN C-terminus, captured on a HSA-coated sensor chip, and human sortilin. (C) Sequence of the PGRN C-terminus, with the peptide denoted PGRN_C21 highlighted. Numbering indicates amino acid numbers from the start codon. Ala588 is shown in green, indicating the position of the A588G mutation in the PGRN_C21* peptide. (D–G) SPR sensorgrams showing the interaction between Z-ABD, Z-ABD-PGRN_C21*, and ABD-Z-PGRN_C21* format constructs and human sortilin, for affibodies G11 (D), F6 (E), C1 (F), and A3 (G), respectively. Due to a low degree of dissociation within the measured 15-minute dissociation time period precluding accurate estimation of kinetic constants, values marked † are low-accuracy approximations.

3.4 Evaluation of first-generation affibody-PGRN fusion constructs

Constructs of the format Z-ABD, Z-ABD-PGRN_C21* and ABD-Z-PGRN_C21* for each of the four sortilin-binding affibodies (Z), as well as ABD-PGRN_C21* were expressed in *E. coli* and purified by IMAC. Potential simultaneous binding to human sortilin by the affibody and PGRN_C21* moieties was investigated by SPR, as described above. Fusion of affibodies G11, C1 and F6 to PGRN_C21* led to limited or no improvements in apparent affinity compared to the parental peptide or affibodies (Figures 2B, D–F), indicating that the affibody and peptide epitopes on sortilin were suboptimal for simultaneous binding. In contrast, fusion of the PGRN_C21* peptide to anti-sortilin affibody A3 led to a dramatic decrease in dissociation rate (Figure 2G), indicating avidity and hence compatibility between the A3 and PGRN_C21* epitopes for simultaneous binding. Notably, the dissociation rate of the A3-PGRN_C21* constructs was too slow to enable accurate determination of kinetic constants within the tested 15-minute dissociation period. Qualitatively, the position of the ABD in the A3-PGRN_C21* constructs seemed to have no major effect on binding, indicating that the ABD moiety was not required as a spacer between A3 and PGRN_C21*. This raised the question of whether parts of the PGRN_C21* peptide also merely acted as a spacer, rather than directly contributing to the co-operative binding.

3.5 Optimization of an affibody-PGRN fusion construct

To investigate whether all 21 amino acids of the PGRN_C21* peptide are required for simultaneous sortilin binding in the A3-PGRN_C fusion protein, constructs of the format ABD-A3-PGRN_CX*, where X={3, 6, 9, 12, 15, 18, 21} (Figure 3A), were produced and purified. The affinities for human sortilin were evaluated by SPR, as described above. Notably, a dramatic difference in dissociation rate and K_D (>13-fold) was seen between the ABD-A3-PGRN_C3 (K_D=3.9 nM) and the ABD-A3-PGRN_C6* (K_D=289 pM) constructs (Figures 3B, C, Table 1), indicating that PGRN_C6* is sufficient to both bind to sortilin and serve as a spacer between the A3 and PGRN_C epitopes. Moreover, a somewhat longer peptide moiety resulted in an even stronger interaction. All tested ABD-A3-PGRN_CX* fusion proteins with a PGRN moiety of 9 or more amino acids had smaller K_D values than ABD-A3-PGRN_C6*, with a minimum K_D value of 185 pM for ABD-A3-PGRN_C15* (Figure 3C, Table 1).

To investigate whether this increase in apparent affinity in A3-PGRN_C constructs with longer PGRN_C peptides was due to the N-terminal amino acids of the PGRN_C moiety interacting with sortilin or merely serving as a spacer, the corresponding amino acids were in additional constructs replaced with a flexible linker. Constructs of the format ABD-A3-(G₄S)₃-PGRN_CX*, where X={3, 6}, were tested for binding to human sortilin in SPR. In contrast to ABD-A3-

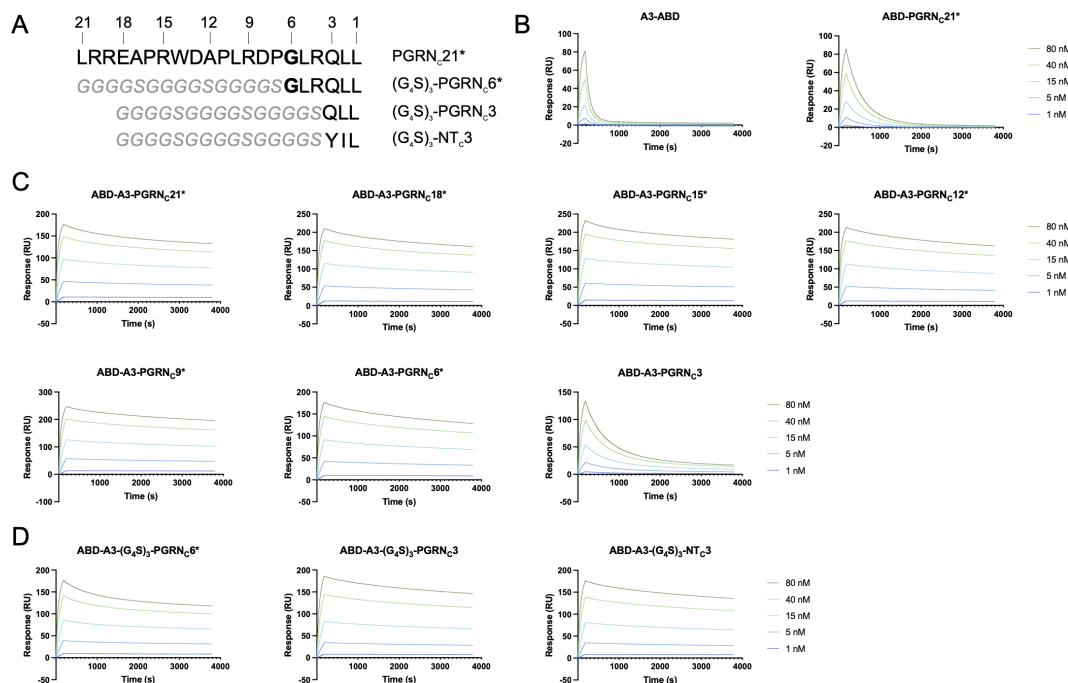


FIGURE 3

SPR-based affinity determination of second-generation A3-PGRN_C fusion proteins. (A) Sequence overview of the various PGRN_C*, (G₄S)₃-PGRN_C*, and (G₄S)₃-NT_{C3} peptides. Numbers indicate the peptide length, as counted from the C-terminus. The site of the PGRN A588G mutation is indicated in bold. (B–D) Representative sensorgrams showing the interaction of the individual affibody and peptide moieties (B), second-generation affibody-peptide fusion constructs (C), and affibody-peptide fusions with a flexible linker (D) with human sortilin. The length of the peptide moieties, according to (A), are indicated in the subfigure headings. ABD-containing constructs were captured on an HSA-coated sensor chip, followed by sortilin injection, and reference subtraction. Displayed sensorgrams are representative examples of n=3 technical replicates.

PGRN_{C3} ($K_D=3.9$ nM), which provided only a modest decrease in K_D versus affibody alone, ABD-A3-(G₄S)₃-PGRN_{C3} ($K_D=310$ pM) had a K_D value in the same range as the fusion proteins with longer PGRN moieties, such as ABD-A3-PGRN_{C6}* ($K_D=289$ pM). This indicates that PGRN_{C3} is sufficient to convey sortilin binding, when spaced appropriately from A3. The very similar apparent K_D values of the ABD-A3-(G₄S)₃-PGRN_{C3} (310 pM) and ABD-A3-(G₄S)₃-PGRN_{C6}* (319 pM) constructs furthermore indicate that the 3 N-terminal-most amino acids of the PGRN_{C6}* peptide (GLR) mainly serve as a spacer in the ABD-A3-PGRN_{C6}* construct, rather than being essential for sortilin binding (Figure 3D, Table 1). However, the higher affinities of ABD-A3-PGRN_{C18}* (217 pM) and ABD-A3-PGRN_{C21}* (215 pM) compared to ABD-A3-(G₄S)₃-PGRN_{C3} (310 pM) and ABD-A3-(G₄S)₃-PGRN_{C6}* (319 pM), respectively, indicate that the N-terminal portion of the longer PGRN_C peptides might in fact contribute somewhat to binding in addition to serving as a spacer.

Additionally, an initial comparison between the 3 C-terminal-most amino acids of the sortilin-binding peptide neurotensin (YIL), known to bind to the same epitope as PGRN (27, 28, 48), and those of PGRN (QLL) was also made, in the form of the construct ABD-A3-(G₄S)₃-NT_{C3}. The ABD-A3-(G₄S)₃-NT_{C3} construct ($K_D=303$ pM) displayed a similar affinity for sortilin as compared to ABD-A3-(G₄S)₃-PGRN_{C3} ($K_D=310$ pM, Figure 3D, Table 1), suggesting

that the QLL and YIL extensions contribute to the sortilin binding with equal potencies.

3.6 Binding to sortilin on cells

Next, the constructs' binding capabilities to sortilin in the more biologically relevant context of the cell surface was investigated. The binding of i) anti-sortilin affibodies, ii) the PGRN C-terminus, iii) A3-PGRN_C fusion proteins, and iv) a negative control affibody (Z_{wt}) to the sortilin high-expressing glioblastoma cell line U-251 and the control prostate cancer cell line PC-3 was compared. Cell line sortilin expression status was verified using a positive control antibody (Supplementary Figure S2). To ensure simultaneous binding to sortilin and HSA, ABD-containing constructs were pre-incubated with an excess of fluorophore-labelled human serum albumin (HSA-Alexa Fluor 647) prior to addition to cells and analysis by flow cytometry. All constructs showed binding to U-251 cells (Figure 4A, Supplementary Figure S3), except the negative control affibody Z_{wt} , which did not show any binding to U-251 or PC-3 cells (Supplementary Figure S2). Notably, the constructs with highest affinities for sortilin also showed a small fluorescence shift relative negative control affibody for the negative control cell line PC-3 (Figure 4A). This is in line with reports of

TABLE 1 Summary of kinetic constants for the interaction of A3-PGRN_C fusion proteins and controls with human sortilin, as determined by SPR.

Construct	Apparent k_{on} (1/Ms)	Apparent k_{off} (1/s)	Apparent K_D (nM)
A3-ABD	$1.16 \times 10^5 \pm 4.64 \times 10^3$	$8.11 \times 10^{-3} \pm 1.10 \times 10^{-4}$	70.4 ± 3.69
ABD-PGRN _C 21*	$2.12 \times 10^5 \pm 6.94 \times 10^3$	$3.37 \times 10^{-3} \pm 5.56 \times 10^{-5}$	15.9 ± 0.22
ABD-A3-PGRN _C 3	$7.52 \times 10^5 \pm 1.84 \times 10^4$	$2.95 \times 10^{-3} \pm 1.41 \times 10^{-5}$	3.93 ± 0.12
ABD-A3-PGRN _C 6*	$2.81 \times 10^5 \pm 4.71 \times 10^2$	$8.09 \times 10^{-5} \pm 1.31 \times 10^{-6}$	0.289 ± 0.0041
ABD-A3-PGRN _C 9*	$2.65 \times 10^5 \pm 4.71 \times 10^2$	$5.95 \times 10^{-5} \pm 9.63 \times 10^{-7}$	0.224 ± 0.0029
ABD-A3-PGRN _C 12*	$2.83 \times 10^5 \pm 4.71 \times 10^2$	$7.12 \times 10^{-5} \pm 1.07 \times 10^{-6}$	0.251 ± 0.0036
ABD-A3-PGRN _C 15*	$3.21 \times 10^5 \pm 2.45 \times 10^3$	$5.94 \times 10^{-5} \pm 8.52 \times 10^{-7}$	0.185 ± 0.0016
ABD-A3-PGRN _C 18*	$3.08 \times 10^5 \pm 1.41 \times 10^3$	$6.69 \times 10^{-5} \pm 8.34 \times 10^{-7}$	0.217 ± 0.0021
ABD-A3-PGRN _C 21*	$3.25 \times 10^5 \pm 1.70 \times 10^3$	$6.98 \times 10^{-5} \pm 1.12 \times 10^{-6}$	0.215 ± 0.0022
ABD-A3-(G ₄ S) ₃ -PGRN _C 3	$2.05 \times 10^5 \pm 5.0 \times 10^2$	$6.34 \times 10^{-5} \pm 7.54 \times 10^{-7}$	0.310 ± 0.0038
ABD-A3-(G ₄ S) ₃ -PGRN _C 6*	$2.88 \times 10^5 \pm 1.63 \times 10^3$	$9.16 \times 10^{-5} \pm 4.55 \times 10^{-7}$	0.319 ± 0.0033
ABD-A3-(G ₄ S) ₃ -NT _C 3	$2.21 \times 10^5 \pm 8.16 \times 10^2$	$6.70 \times 10^{-5} \pm 8.34 \times 10^{-7}$	0.303 ± 0.0047

Values for k_{on} , k_{off} and K_D were obtained from a 1:1 Langmuir curve fit of reference subtracted sensorgrams. Values are given as mean \pm SD from n=3 technical replicates.

* indicates the presence of the A588G mutation in PGRN-derived peptides.

some low sortilin expression on PC-3 cells, as determined by western blot (49), and the high affinity of these constructs for sortilin.

3.7 Effect on extracellular PGRN levels *in vitro*

The biological activity of affibody-PGRN_C peptide fusions was evaluated in a cell-based progranulin clearance assay. U-251 cells both express sortilin and secrete progranulin, making them a suitable model system to study the effect of sortilin binders on extracellular PGRN levels. The ABD-A3-PGRN_C15* construct, showing the highest affinity for sortilin in SPR, was chosen as the lead affibody-peptide fusion candidate, and evaluated in comparison to i) A3 alone, ii) the PGRN C-terminus alone, iii) an affibody negative control (Z_{wt}), and iv) latozinemab. Under the employed experimental conditions, supernatant PGRN levels in untreated cells, constituting the baseline, were 1.52 ± 0.15 ng/ml. At the highest tested concentration (500 nM), A3 and PGRN_C alone did not reach more than a 1.48 ± 0.31 - and 1.44 ± 0.27 -fold increase in extracellular PGRN levels compared to untreated cells, respectively, with the lack of a plateau making EC_{50} determination unreliable. In contrast, ABD-A3-PGRN_C15* increased extracellular

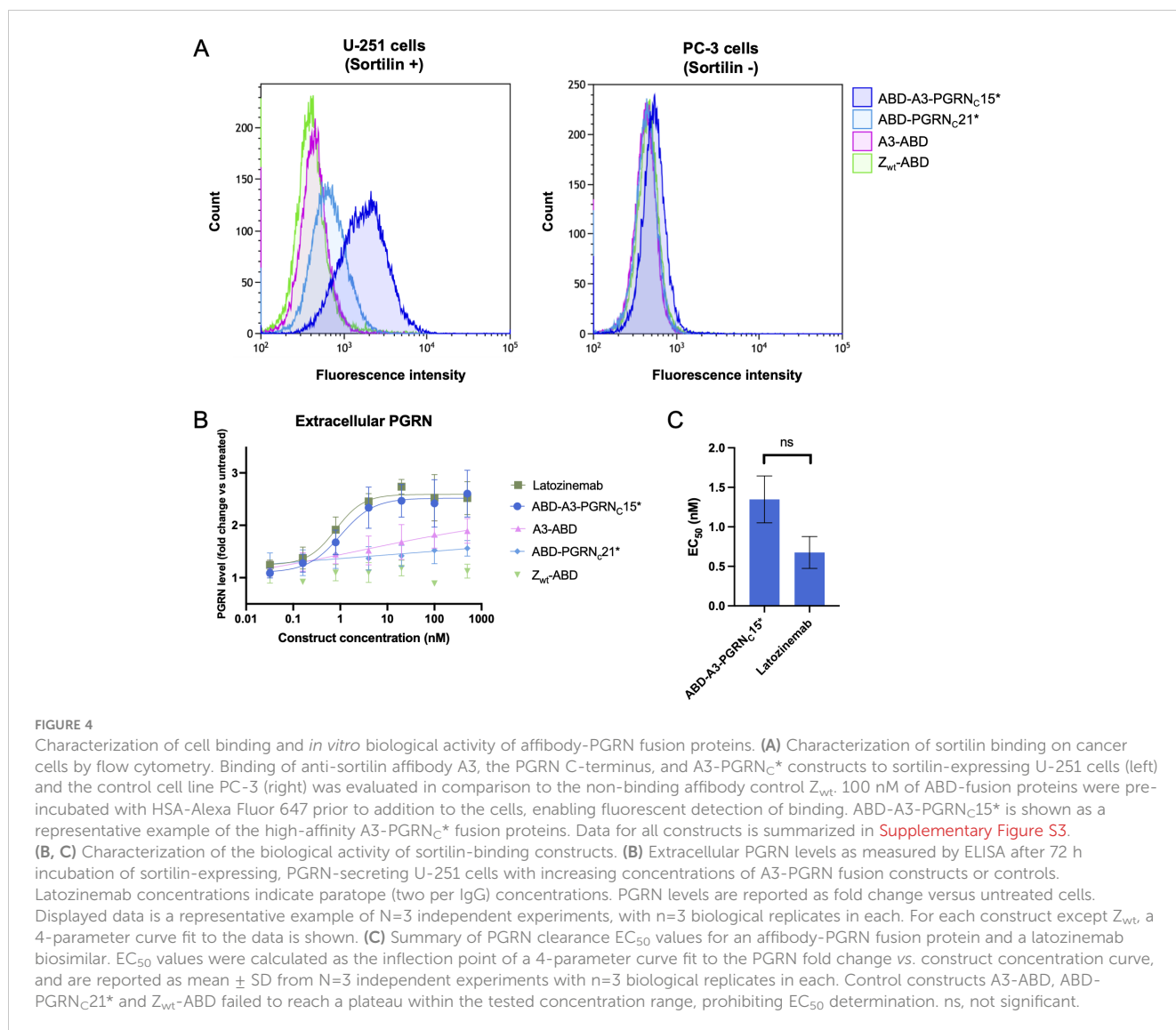
PGRN levels 2.50 ± 0.19 -fold compared to untreated cells, with an EC_{50} value of 1.30 ± 0.30 nM. Notably, this is comparable to the 2.42 ± 0.12 -fold increase and EC_{50} of 0.68 ± 0.20 nM of latozinemab (Figures 4B, C). The difference in EC_{50} values between ABD-A3-PGRN_C15* and latozinemab was not statistically significant ($p=0.19$).

4 Discussion

Heterozygous loss-of-function mutations in the *GRN* gene lead to FTD through haploinsufficiency (9, 22). Blocking the interaction of PGRN with its clearance receptor sortilin has emerged as a promising therapeutic strategy for FTD-*GRN*, by normalizing the extracellular PGRN levels. To this end, we aimed to develop a high-affinity sortilin-binding affibody-peptide fusion construct, utilizing the fact that PGRN interacts with sortilin through the PGRN C-terminus. Affibody molecules against sortilin were selected by phage display, and later genetically fused with peptides derived from the PGRN C-terminus. For the anti-sortilin affibody A3, fusion with the PGRN C-terminus demonstrated avidity effects and a significantly decreased dissociation rate, indicating that the A3 and PGRN_C epitopes are compatible for simultaneous binding to sortilin. Optimization of the peptide moiety of the A3-PGRN_C fusion construct, as summarized in Figure 3, enabled an up to 380-fold improvement in K_D of the fusion construct compared to the parental affibody alone.

In line with previous findings (29), the optimization of the A3-PGRN_C fusion construct shows that the very C-terminal-most amino acids of PGRN are sufficient to convey sortilin binding (ABD-A3-PGRN_C6*), while a slightly longer peptide yields a higher affinity of the fusion construct (e.g. ABD-A3-PGRN_C15*). Our results, however, indicate that the N-terminal amino acids of these PGRN-derived peptides mainly serve as a spacer, with the PGRN_C3 peptide harboring the key residues for sortilin binding, as PGRN_C3 with a flexible linker conveys a similar binding contribution to PGRN_C6* (ABD-A3-(G₄S)₃-PGRN_C3 vs. ABD-A3-(G₄S)₃-PGRN_C6*). This is furthermore in agreement with the A588G mutation not affecting the PGRN affinity for sortilin (33), and indicates that the N-terminal amino acids of the optimal fusion peptide PGRN_C15* might be amenable to further mutations, for instance to increase stability of the fusion construct *in vivo*.

To investigate the potential of the fusion construct as an FTD-*GRN* therapeutic candidate, the biological activity of A3-PGRN_C15* was evaluated in a PGRN clearance assay, with latozinemab as comparator. Incubation of sortilin-expressing, PGRN-secreting human glioblastoma U-251 cells with A3-PGRN_C15* increased the extracellular PGRN levels to the same extent as latozinemab, with an EC_{50} value in the same concentration range. While it should be noted that the biosimilar used in this study may differ from the antibody used in clinical trials, and that the lack of statistically significant difference in EC_{50} values may be an effect of limited statistical power, this nonetheless provides an indication that A3-PGRN_C15* has an affinity and binding mode suitable for the intended application. It should furthermore be noted that higher affinity of the A3 affibody moiety might be possible to achieve through affinity maturation procedures. Further studies in more



biologically relevant FTD models are required to further elucidate the potential of A3-PGRN_C15* as a therapeutic candidate.

Since their invention, affibody molecules have been investigated extensively for various medical applications [reviewed in (50, 51)]. A therapeutic strategy based on affibody molecules for treatment of FTD-GRN would provide an orthogonal approach to the antibody therapies currently under investigation, broadening the spectrum of potential sortilin-targeting therapies. Furthermore, the small size of affibody molecules entails a higher binding site density compared to antibodies, enabling smaller injected volumes and faster administration, likely with similar brain uptake (52–54). In the general case of dementia, and specifically in the case of the genetic FTD-GRN, decades-long treatments will most likely be required, making ease of administration and production costs essential factors. The recent approvals of Alzheimer's disease (AD) antibody drugs aducanumab, lecanemab and donanemab have sparked debate about prohibitive costs in relation to risk/benefit assessments of new dementia therapies. In this context, the bacterial production or chemical synthesis of affibody molecules may provide an attractive option.

The sortilin-binding A3-PGRN_C fusion constructs have here been investigated in the context of FTD-GRN, but manipulation of the sortilin-PGRN axis might also be of interest in other conditions. There are indications that GRN mutations may play a role in other neurodegenerative diseases, such as amyotrophic lateral sclerosis (55), Parkinson's disease (56), and AD (57–61), with increased PGRN levels having been shown to inhibit plaque formation and protect against amyloid beta toxicity in mouse models of AD (62, 63). Furthermore, there is evidence indicating that blocking the sortilin-neurotensin or sortilin-progranulin interactions might be of interest for the treatment of neuropathic pain (64) and certain forms of breast cancer (65, 66), respectively. Thus, the constructs presented here may have wider applicability than to FTD-GRN only.

The present work constitutes the first example of a fusion protein between a peptide and an affibody molecule directed towards the same target, utilizing a combination of directed evolution and naturally occurring receptor ligands to develop high-affinity binders. This approach constitutes an efficient way of greatly increasing the apparent affinity of a binder, and decreasing

the need for extensive affinity maturation efforts. While requiring evaluation on a case-by-case basis, the approach could easily be extended to introduce the peptide moiety in the affibody selections. Whereas more established methods of increasing target affinity, such as classic affinity maturation or creation of biparatopic dimeric affibody constructs, have often been successful, the here presented method constitutes an addition to this toolbox of approaches, that may be used in certain cases.

Data availability statement

The original contributions presented in the study are included in the article/Supplementary Material. Further inquiries can be directed to the corresponding author.

Ethics statement

Ethical approval was not required for the studies on humans in accordance with the local legislation and institutional requirements because only commercially available established cell lines were used.

Author contributions

ME: Writing – original draft, Validation, Methodology, Investigation, Formal analysis, Data curation, Writing – review & editing, Visualization, Conceptualization. JN: Writing – original draft, Writing – review & editing, Investigation, Formal analysis. P-ÅN: Visualization, Conceptualization, Writing – review & editing. SS: Supervision, Resources, Funding acquisition, Writing – review & editing, Conceptualization. HL: Writing – review & editing, Supervision, Conceptualization. JL: Visualization, Resources, Project administration, Funding acquisition, Writing – review & editing, Supervision, Conceptualization.

References

- Vieira RT. Epidemiology of early-onset dementia: a review of the literature. *Clin Pract Epidemiol Ment Health*. (2013) 9:88–95. doi: 10.2174/1745017901309010088
- Rosen HJ, Gorno-Tempini ML, Goldman WP, Perry RJ, Schuff N, Weiner M, et al. Patterns of brain atrophy in frontotemporal dementia and semantic dementia. *Neurology*. (2002) 58:198–208. doi: 10.1212/WNL.58.2.198
- Bang J, Spina S, Miller BL. Frontotemporal dementia. *Lancet*. (2015) 386:1672–82. doi: 10.1016/S0140-6736(15)00461-4
- Rohrer JD, Guerreiro R, Vandrovicova J, Uphill J, Reiman D, Beck J, et al. The heritability and genetics of frontotemporal lobar degeneration. *Neurology*. (2009) 73:1451–6. doi: 10.1212/WNL.0b013e3181bf997a
- Po K, Leslie FVC, Gracia N, Bartley L, Kwok JBJ, Halliday GM, et al. Heritability in frontotemporal dementia: more missing pieces? *J Neurol*. (2014) 261:2170–7. doi: 10.1007/s00415-014-7474-9
- Seelaar H, Kamphorst W, Rosso SM, Azmani A, Masdjedi R, De Koning I, et al. Distinct genetic forms of frontotemporal dementia. *Neurology*. (2008) 71:1220–6. doi: 10.1212/01.wnl.0000319702.37497.72
- Moore KM, Nicholas J, Grossman M, McMillan CT, Irwin DJ, Massimo L, et al. Age at symptom onset and death and disease duration in genetic frontotemporal dementia: an international retrospective cohort study. *Lancet Neurol*. (2020) 19:145–56. doi: 10.1016/S1474-4422(19)30394-1
- Pickering-Brown SM, Rollinson S, Du Plessis D, Morrison KE, Varma A, Richardson AMT, et al. Frequency and clinical characteristics of progranulin mutation carriers in the Manchester frontotemporal lobar degeneration cohort: Comparison with patients with MAPT and no known mutations. *Brain*. (2008) 131:721–31. doi: 10.1093/brain/awm331
- Cruts M, Gijselinck I, van der Zee J, Engelborghs S, Wils H, Pirici D, et al. Null mutations in progranulin cause ubiquitin-positive frontotemporal dementia linked to chromosome 17q21. *Nature*. (2006) 442:920–4. doi: 10.1038/nature05017
- Gass J, Cannon A, Mackenzie IR, Boeve B, Baker M, Adamson J, et al. Mutations in progranulin are a major cause of ubiquitin-positive frontotemporal lobar degeneration. *Hum Mol Genet*. (2006) 15:2988–3001. doi: 10.1093/hmg/ddl241
- Le Ber I, van der Zee J, Hannequin D, Gijselinck I, Campion D, Puel M, et al. Progranulin null mutations in both sporadic and familial frontotemporal dementia. *Hum Mutation*. (2007) 28:846–55. doi: 10.1002/humu.v28:9
- Bhandari V, Palfrey RGE, Bateman A. Isolation and sequence of the granulin precursor cDNA from human bone marrow reveals tandem cysteine-rich granulin domains. *Proc Natl Acad Sci U S A*. (1992) 89:1715–9. doi: 10.1073/pnas.89.5.1715
- Bateman A, Bennett HPJ. Granulins: The structure and function of an emerging family of growth factors. *J Endocrinol*. (1998) 158:145–51. doi: 10.1677/joe.0.1580145

Funding

The author(s) declare financial support was received for the research, authorship, and/or publication of this article. This work was supported primarily by grants from Hjärnfonden FO2022-0253, FO2023-0141, as well as by grants from the Knut and Alice Wallenberg Foundation (grants KAW 2021.0197, KAW 2023.0369 and KAW 2019.0341 for the Wallenberg Center for Protein Research - WCPR), as well as from Hjärnfonden FO2021-0407, FO2023-0400, the Swedish Research Council (2019–05115); StratNeuro, and the Swedish Agency for Innovation VINNOVA (2019/00104 and CellNova center; 2017/02105).

Conflict of interest

HL, P-ÅN, SS and JL are shareholders of Amylonix AB.

The remaining authors declare that the research was conducted in the absence of any commercial or financial relationships that could be construed as a potential conflict of interest.

Publisher's note

All claims expressed in this article are solely those of the authors and do not necessarily represent those of their affiliated organizations, or those of the publisher, the editors and the reviewers. Any product that may be evaluated in this article, or claim that may be made by its manufacturer, is not guaranteed or endorsed by the publisher.

Supplementary material

The Supplementary Material for this article can be found online at: <https://www.frontiersin.org/articles/10.3389/fimmu.2024.1437886/full#supplementary-material>

14. Bateman A, Belcourt D, Bennett H, Lazure C, Solomon S. Granulins, a novel class of peptide from leukocytes. *Biochem Biophys Res Commun.* (1990) 173:1161–8. doi: 10.1016/S0006-291X(05)80908-8
15. Lee CW, Stankowski JN, Chew J, Cook CN, Lam YW, Almeida S, et al. The lysosomal protein cathepsin L is a progranulin protease. *Mol Neurodegener.* (2017) 12:1–9. doi: 10.1186/s13024-017-0196-6
16. Zhu J, Nathan C, Jin W, Sim D, Ashcroft GS, Wahl SM, et al. Conversion of proepithelin to epithelins. *Cell.* (2002) 111:867–78. doi: 10.1016/S0092-8674(02)01141-8
17. Tanaka Y, Suzuki G, Matsuwaki T, Hosokawa M, Serrano G, Beach TG, et al. Progranulin regulates lysosomal function and biogenesis through acidification of lysosomes. *Hum Mol Genet.* (2017) 26:969–88. doi: 10.1093/hmg/ddx011
18. Logan T, Simon MJ, Rana A, Chert GM, Srivastava A, Davis SS, et al. Rescue of a lysosomal storage disorder caused by Grn loss of function with a brain penetrant progranulin biologic. *Cell.* (2021) 184:4651–4668.e25. doi: 10.1016/j.cell.2021.08.002
19. Van Damme P, Van Hoecke A, Lambrechts D, Vanacker P, Bogaert E, Van Swieten J, et al. Progranulin functions as a neurotrophic factor to regulate neurite outgrowth and enhance neuronal survival. *J Cell Biol.* (2008) 181:37–41. doi: 10.1083/jcb.200712039
20. De Muynck L, Herdewyn S, Beel S, Scheveneels W, Van Den Bosch L, Robberecht W, et al. The neurotrophic properties of progranulin depend on the granulin E domain but do not require sortilin binding. *Neurobiol Aging.* (2013) 34:2541–7. doi: 10.1016/j.neurobiolaging.2013.04.022
21. Gass J, Lee WC, Cook C, Finch N, Stetler C, Jansen-West K, et al. Progranulin regulates neuronal outgrowth independent of Sortilin. *Mol Neurodegener.* (2012) 7:1–13. doi: 10.1186/1750-1326-7-33
22. Baker M, Mackenzie IR, Pickering-Brown SM, Gass J, Rademakers R, Lindholm C, et al. Mutations in progranulin cause tau-negative frontotemporal dementia linked to chromosome 17. *Nature.* (2006) 442:916–9. doi: 10.1038/nature05016
23. Meeter LHH, Patzke H, Loewen G, Dopfer EGP, Pijnenburg YAL, Van Minkelen R, et al. Progranulin levels in plasma and cerebrospinal fluid in granulin mutation carriers. *Dement Geriatr Cognit Dis Extra.* (2016) 6:330–40. doi: 10.1159/000447738
24. Finch N, Baker M, Crook R, Swanson K, Kuntz K, Surtees R, et al. Plasma progranulin levels predict progranulin mutation status in frontotemporal dementia patients and asymptomatic family members. *Brain.* (2009) 132:583–91. doi: 10.1093/brain/awn352
25. Ghidoni R, Benussi L, Glionna M, Franzoni M, Binetti G. Low plasma progranulin levels predict progranulin mutations in frontotemporal lobar degeneration. *Neurology.* (2008) 71:1235–9. doi: 10.1212/01.wnl.0000325058.10218.fc
26. Petersen CM, Nielsent MS, Nykjaer A, Jacobsen L, Tommerup N, Rasmussen HH, et al. Molecular identification of a novel candidate sorting receptor purified from human brain by receptor-associated protein affinity chromatography. *J Biol Chem.* (1997) 272:3599–605. doi: 10.1074/jbc.272.6.3599
27. Quistgaard EM, Madsen P, Grøftehaug MK, Nissen P, Petersen CM, Thirup SS. Ligands bind to Sortilin in the tunnel of a ten-bladed β -propeller domain. *Nat Struct Mol Biol.* (2009) 16:96–8. doi: 10.1038/nsmb.1543
28. Hu F, Padukkavidana T, Vægter CB, Brady OA, Zheng Y, Mackenzie IR, et al. Sortilin-mediated endocytosis determines levels of the frontotemporal dementia protein, progranulin. *Neuron.* (2010) 68:654–67. doi: 10.1016/j.neuron.2010.09.034
29. Zheng Y, Brady OA, Meng PS, Mao Y, Hu F. C-terminus of progranulin interacts with the beta-propeller region of sortilin to regulate progranulin trafficking. *PLoS One.* (2011) 6(6):e21023. doi: 10.1371/journal.pone.0021023
30. Carrasquillo MM, Nicholson AM, Finch N, Gibbs JR, Baker M, Rutherford NJ, et al. Genome-wide screen identifies rs646776 near sortilin as a regulator of progranulin levels in human plasma. *Am J Hum Genet.* (2010) 87:890–7. doi: 10.1016/j.ajhg.2010.11.002
31. Miyakawa S, Sakuma H, Warude D, Asanuma S, Arimura N, Yoshihara T, et al. Anti-sortilin1 antibody up-regulates progranulin via sortilin1 down-regulation. *Front Neurosci.* (2020) 14. doi: 10.3389/fnins.2020.586107
32. Kurnellas M, Mitra A, Schwabe T, Paul R, Arrant AE, Roberson ED, et al. Latozinemab, a novel progranulin - elevating therapy for frontotemporal dementia. *J Transl Med.* (2023) 21:1–18. doi: 10.1186/s12967-023-04251-y
33. Lee WC, Almeida S, Prudencio M, Caulfield TR, Zhang YJ, Tay WM, et al. Targeted manipulation of the sortilin-progranulin axis rescues progranulin haploinsufficiency. *Hum Mol Genet.* (2014) 23:1467–78. doi: 10.1093/hmg/ddt534
34. Simeon R, Chen Z. *In vitro*-engineered non-antibody protein therapeutics. In: *Protein and cell.* (2019) 9:3–14. doi: 10.1007/s13238-017-0386-6
35. Nilsson B, Moks T, Jansson B, Abrahamssén L, Elmlblad A, Holmgren E, et al. A synthetic IgG-binding domain based on staphylococcal protein A. *Protein Eng Design Selection.* (1987) 1:107–13. doi: 10.1093/protein/1.2.107
36. Uhlén M, Guss B, Nilsson B, Gatenbeck S, Philipson L, Lindberg M. Complete sequence of the staphylococcal gene encoding protein A. *J Biol Chem.* (1984) 259:1695–702. doi: 10.1016/S0021-9258(17)43463-6
37. Nord K, Gunneriusson E, Ringdahl J, Ståhl S, Uhlén M, Nygren PÅ. Binding proteins selected from combinatorial libraries of an α -helical bacterial receptor domain. *Nat Biotechnol.* (1997) 15:772–7. doi: 10.1038/nbt0897-772
38. Fleetwood F, Klint S, Hanze M, Gunneriusson E, Frejd FY, Ståhl S, et al. Simultaneous targeting of two ligand-binding sites on VEGFR2 using biparatopic Affibody molecules results in dramatically improved affinity. *Sci Rep.* (2014) 4:1–14. doi: 10.1038/srep07518
39. Roy S, Curry SD, Corbella Bagot C, Mueller EN, Mansouri AM, Park W, et al. Enzyme prodrug therapy with photo-cross-linkable anti-EGFR affibodies conjugated to upconverting nanoparticles. *ACS Nano.* (2022) 16:15873–83. doi: 10.1021/acsnano.2c02558
40. Lan KH, Tsai CL, Chen YY, Lee TL, Pai CW, Chao Y, et al. Affibody-conjugated 5-fluorouracil prodrug system preferentially targets and inhibits HER2-expressing cancer cells. *Biochem Biophys Res Commun.* (2021) 582:137–43. doi: 10.1016/j.bbrc.2021.09.078
41. Mestre Borrás A, Dahlsson Leitao C, Ståhl S, Löfblom J. Generation of an anti-idiotypic affibody-based masking domain for conditional activation of EGFR-targeting. *N Biotechnol.* (2023) 73:9–18. doi: 10.1016/j.nbt.2022.12.002
42. Sandersjö L, Jonsson A, Löfblom J. A new prodrug form of Affibody molecules (pro-Affibody) is selectively activated by cancer-associated proteases. *Cell Mol Life Sci.* (2015) 72:1405–15. doi: 10.1007/s00018-014-1751-8
43. Andersen JT, Pehrson R, Tolmachev V, Daba MB, Abrahamssén L, Ekblad C. Extending half-life by indirect targeting of the neonatal Fc receptor (FcRn) using a minimal albumin binding domain. *J Biol Chem.* (2011) 286:5234–41. doi: 10.1074/jbc.M110.164848
44. Klint S, Feldwisch J, Gudmundsdóttir L, Dillner Bergstedt K, Gunneriusson E, Höiden Guttenberg I, et al. Izokibep: Preclinical development and first-in-human study of a novel IL-17A neutralizing Affibody molecule in patients with plaque psoriasis. *MAbs.* (2023) 15(1). doi: 10.1080/19420862.2023.2209920
45. Giang KA, Nygren PÅ, Nilvebrant J. Selection of affibody affinity proteins from phagemid libraries. In: Hust M, Lim TS, editors. *Phage Display Methods in Molecular Biology, 2nd ed., vol. 2702.* Humana, New York, NY (2023). p. 373–92.
46. Giang KA, Boxaspen T, Diao Y, Nilvebrant J, Kosugi-Kanaya M, Kanaya M, et al. Affibody-based hBCMA x CD16 dual engagers for NK cell-mediated killing of multiple myeloma cells. *N Biotechnol.* (2023) 77:139–48. doi: 10.1016/j.nbt.2023.09.002
47. Jonsson A, Dogan J, Herne N, Abrahamssén L, Nygren PÅ. Engineering of a femtomolar affinity binding protein to human serum albumin. *Protein Eng Design Selection.* (2008) 21:515–27. doi: 10.1093/protein/gzn028
48. Trabjerg E, Abu-Asad N, Wan Z, Kartberg F, Christensen S, Rand KD. Investigating the conformational response of the sortilin receptor upon binding endogenous peptide- and protein ligands by HDX-MS. *Structure.* (2019) 27:1103–1113.e3. doi: 10.1016/j.str.2019.04.006
49. Tanimoto R, Morcavallo A, Terracciano M, Xu SQ, Stefanello M, Buraschi S, et al. Sortilin regulates progranulin action in castration-Resistant prostate cancer cells. *Endocrinology.* (2015) 156:58–70. doi: 10.1210/en.2014-1590
50. Löfblom J, Feldwisch J, Tolmachev V, Carlsson J, Ståhl S, Frejd FY. Affibody molecules: Engineered proteins for therapeutic, diagnostic and biotechnological applications. *FEBS Lett.* (2010) 584:2670–80. doi: 10.1016/j.febslet.2010.04.014
51. Ståhl S, Gräslund T, Eriksson Karlström A, Frejd FY, Nygren PÅ, Löfblom J. Affibody molecules in biotechnological and medical applications. *Trends Biotechnol.* (2017) 35:691–712. doi: 10.1016/j.tibtech.2017.04.007
52. Meister SW, Hjelm LC, Dannemeyer M, Tegel H, Lindberg H, Ståhl S, et al. An affibody molecule is actively transported into the cerebrospinal fluid via binding to the transferrin receptor. *Int J Mol Sci.* (2020) 21:1–14. doi: 10.3390/ijms21082999
53. Boutajangout A, Lindberg H, Awwad A, Paul A, Baitalmal R, Almqoyad I, et al. Affibody-mediated sequestration of amyloid β demonstrates preventive efficacy in a transgenic Alzheimer's disease mouse model. *Front Aging Neurosci.* (2019) 11:1–13. doi: 10.3389/fnagi.2019.00064
54. Wang Q, Delva L, Weinreb PH, Pepinsky RB, Graham D, Veizaj E, et al. Monoclonal antibody exposure in rat and cynomolgus monkey cerebrospinal fluid following systemic administration. *Fluids Barriers CNS.* (2018) 15:1–10. doi: 10.1186/s12987-018-0093-6
55. Slegers K, Brouwers N, Maurer-Stroh S, Van Es MA, Van Damme P, Van Vught PWJ, et al. Progranulin genetic variability contributes to amyotrophic lateral sclerosis. *Neurology.* (2008) 71:253–9. doi: 10.1212/01.wnl.0000289191.54852.75
56. Nalls MA, Blauwendraat C, Vallerga CL, Heilbron K, Bandres-Ciga S, Chang D, et al. Identification of novel risk loci, causal insights, and heritable risk for Parkinson's disease: a meta-genome wide association study. *Lancet Neurol.* (2019) 18:1091–102. doi: 10.1016/S1474-4422(19)30320-5
57. Cortini F, Fenoglio C, Guidi I, Venturelli E, Pomati S, Marcone A, et al. Novel exon 1 progranulin gene variant in Alzheimer's disease. *Eur J Neurol.* (2008) 15:1111–7. doi: 10.1111/j.1468-1331.2008.02266.x
58. Perry DC, Lehmann M, Yokoyama JS, Karydas A, Lee JYY, Coppola G, et al. Progranulin mutations as risk factors for Alzheimer disease. *JAMA Neurol.* (2013) 70:774–8. doi: 10.1001/2013.jamaneurol.393
59. Lee MJ, Chen TF, Cheng TW, Chiu MJ. rs5848 variant of progranulin gene is a risk of Alzheimer's disease in the Taiwanese population. *Neurodegener Dis.* (2011) 8:216–20. doi: 10.1159/000322538
60. Sheng J, Su L, Xu Z, Chen G. Progranulin polymorphism rs5848 is associated with increased risk of Alzheimer's disease. *Gene.* (2014) 542:141–5. doi: 10.1016/j.gene.2014.03.041
61. Brouwers N, Slegers K, Engelborghs S, Maurer-Stroh S, Gijssels I, van der Zee J, et al. Genetic variability in progranulin contributes to risk for clinically diagnosed Alzheimer disease. *Neurology.* (2008) 71:656–64. doi: 10.1212/01.wnl.0000319688.89790.7a
62. Minami SS, Min SW, Krabbe G, Wang C, Zhou Y, Asgarov R, et al. Progranulin protects against amyloid β deposition and toxicity in Alzheimer's disease mouse models. *Nat Med.* (2014) 20:1157–64. doi: 10.1038/nm.3672
63. Van Kampen JM, Kay DG. Progranulin gene delivery reduces plaque burden and synaptic atrophy in a mouse model of Alzheimer's disease. *PLoS One.* (2017) 12:1–22. doi: 10.1371/journal.pone.0182896
64. Richner M, Pallesen LT, Ulrichsen M, Poulsen ET, Holm TH, Login H, et al. Sortilin gates neurotensin and BDNF signaling to control peripheral neuropathic pain. *Sci Adv.* (2019) 5:eav9946. doi: 10.1126/sciadv.aav9946

65. Rhost S, Hughes É, Harrison H, Rafnsdottir S, Jacobsson H, Gregersson P, et al. Sortilin inhibition limits secretion-induced progranulin-dependent breast cancer progression and cancer stem cell expansion. *Breast Cancer Res.* (2018) 20:1–15. doi: 10.1186/s13058-018-1060-5

66. Berger K, Pauwels E, Parkinson G, Landberg G, Le T, Demillo VG, et al. Reduction of progranulin-induced breast cancer stem cell propagation by sortilin-targeting cyclotriazadisulfonamide (CADA) compounds. *J Med Chem.* (2021) 64:12865–76. doi: 10.1021/acs.jmedchem.1c00943